EEET ECOLOGICAL ENGINEERING & ENVIRONMENTAL TECHNOLOGY

Ecological Engineering & Environmental Technology, 2026, 27(9), 482–495
https://doi.org/10.12912/27197050/226762
ISSN 2719–7050, License CC-BY 4.0

Received: 2026.07.17
Accepted: 2026.08.03
Published: 2026.08.15

Continuous-flow magnesium-activated biochar filtration for ammonium and phosphate recovery from domestic wastewater

I Made Wahyu Wijaya[1*], Nurul Setiadewi[2], Ni Made Dharma Shantini Suena[3], I Ketut Sumantra[4], Dewa Agung Dibyacitta[5], Filemon Bram Gunas Junior[5]

[1] Regional and Rural Planning Study Program, Postgraduate Program, Universitas Mahasaraswati Denpasar, Denpasar, Indonesia
[2] Research Center for Limnology and Water Resources, National Research and Innovation Agency, Indonesia
[3] Pharmacy Study Program, Faculty of Pharmacy, Universitas Mahasaraswati Denpasar, Denpasar, Indonesia
[4] Agrotechnology Study Program, Faculty of Agriculture and Business, Universitas Mahasaraswati Denpasar, Denpasar, Indonesia
[5] Environmental Engineering Study Program, Faculty of Engineering, Universitas Mahasaraswati Denpasar, Denpasar, Indonesia
* Corresponding author's e-mail: wijaya@unmas.ac.id

ABSTRACT

Excess nitrogen and phosphorus in domestic wastewater accelerate eutrophication, yet many biochar-based nutrient studies remain dominated by batch tests with limited evidence under continuous-flow conditions relevant to real treatment units. Magnesium-activated biochar was packed into laboratory-scale columns and operated under continuous flow while systematically varying bed depth (25 vs 50 cm) and hydraulic configuration. Treatment performance was monitored through influent–effluent nutrient measurements over extended operation, supported by hydraulic assessment (hydraulic retention time, permeability via Darcy analysis) and surface characterization using SEM before and after filtration. Across all configurations, Mg^{2+}-activated biochar removed ammonium effectively, with peak removal of 76.69–79.15% achieved within 8–9 days of operation across all four configurations, followed by a partial decline (overall trial means ranging 37.91–56.29% depending on configuration). The best-performing setup (50 cm, downflow–upflow) reached the highest single-day removal of 79.15% (46.58 mg/L) on day 8 and the highest overall mean removal (56.29% ± 15.28%) across the trial. In contrast, phosphate removal was strongly configuration-dependent: the 25 cm downflow configuration sustained stable removal (65.03% ± 10.29%) throughout the trial, while the remaining three configurations showed unstable behavior, with effluent concentrations frequently exceeding influent values, suggesting desorption/leaching and/or biologically mediated accumulation, and underscoring the importance of filter configuration as an operational control. Hydraulically, the system achieved an estimated HRT of ~16 h at 25 mL/min, and thicker media exhibited higher permeability (0.001161 vs 0.000714 cm/s). SEM revealed substantial pore blockage and fouling after operation, consistent with coupled physical filtration and chemical adsorption processes. Overall, Mg^{2+}-activated biochar filtration shows strong promise for ammonium polishing with clear configuration-dependent performance gains, while phosphate management requires targeted operating strategies to prevent desorption and enable reliable recovery under continuous flow.

Keywords: adsorption, ammonium, biochar, filtration, nutrient, phosphate, wastewater.

INTRODUCTION

Nutrient enrichment from domestic wastewater remains one of the most persistent pressures on freshwater and coastal ecosystems. Reactive nitrogen (N) and phosphorus (P) stimulate excessive primary production and can trigger harmful algal blooms (Ural-Janssen et al., 2024), hypoxia, and biodiversity loss, especially where nutrient loads are continuous and receiving waters have limited assimilative capacity (Kundu et al., 2015; Panjwani, Cowan et al., 2021). In many developing and rapidly urbanizing contexts, eutrophication risks are compounded by variable treatment performance and legacy sources such as phosphate-containing detergents, which increase P loading to surface waters (Ricklefs-Johnson et al., 2023; Wijaya et al., 2023). As a result, nutrient control is increasingly framed as both an environmental protection priority and a requirement for resilient water infrastructure.

At the same time, the sector's narrative is shifting from end-of-pipe "pollutant removal" toward circular approaches that treat wastewater as a circular resource stream (Nika et al., 2020; Slootweg, 2020). Nutrient capture and reuse are central to this transition because N and P are essential for food systems yet problematic when discharged unmanaged (Balkrishna et al., 2025; Hartati et al., 2025; Marcińczyk et al., 2022). The practical implication is a growing demand for technologies that are robust under dynamic wastewater characteristic, simple to operate, and capable of concentrating nutrients into a solid phase that can be handled, recovered, or potentially valorised (Nehhal et al., 2025; Rey-Martínez et al., 2024). These needs are particularly relevant for decentralized and polishing applications, where compact modular units can complement biological processes or provide downstream stabilization of effluent quality (Hofmann et al., 2024; Wijaya et al., 2025).

Conventional biological and chemical nutrient-removal processes can be effective, but they often require specific operational control and continuous chemical inputs, and they(Czuba et al., 2021; Wu et al., 2025; Wu and Vaneeckhaute, 2022) do not always support straightforward nutrient recovery. These limitations have renewed interest in adsorption and filtration, which offer a simple, modular polishing step that can be retrofitted to existing treatment trains and can concentrate nutrients for potential recovery or reuse (Yu et al., 2014; Zakrisson et al., 2024). Biochar has emerged as a promising adsorption medium due to its low-cost feedstock options, tuneable porosity and surface chemistry, and its alignment with broader carbon-management and waste valorisation goals. Recent reviews synthesize a rapidly expanding biochar literature and emphasize that pollutant removal depends strongly on feedstock, pyrolysis conditions, and post-treatment/activation, with key mechanisms including ion exchange, surface complexation, pore filling, and precipitation (Mahmoud, 2018; Perez-Mercado et al., 2019; Reddy et al., 2014; Zakrisson et al., 2024). For nutrient control, pristine biochar often shows inconsistent uptake prompting substantial attention to engineered biochar modified with metals/minerals, chemical activation, and functionalization to increase selectivity and capacity (Goldschmidt and Buffam, 2023; Quispe et al., 2022).

Magnesium modification is especially attractive for nutrient applications because Mg^{2+} ion can enhance cation exchange and create reactive surfaces that support complexation and precipitation pathways relevant to both ammonium and phosphate (Ha et al., 2023; I. Wijaya, 2025; Xu et al., 2018). Comparative studies of Mg-loaded biochar produced from different feedstocks have shown measurable N and P adsorption, while highlighting the importance of material properties and water chemistry in controlling removal pathways and capacities (Xu et al., 2018). Phosphate binding is sensitive to pH and competing anions, and modified biochar can exhibit sharply different performance across operational windows (Gong et al., 2017; Reddy et al., 2025). Moreover, the emerging literature increasingly connects nutrient recovery including approaches where nutrient-laden biochar is evaluated for fertilizer-related applications, if capture is stable and product safety can be demonstrated (Gong et al., 2017; Ren et al., 2023; Xu et al., 2018). However, this evidence base is dominated by short-term batch isotherm and kinetic experiment, including the two most directly comparable Mg-loaded biochar studies (Jiang et al., 2019; Xu et al., 2018), conducted under equilibrium-shaking conditions with synthetic solutions or urine rather than continuous flow through a packed bed. How Mg^{2+}-activated biochar performs when ammonium and phosphate must be captured simultaneously from real domestic wastewater percolating through a fixed bed, where contact time, flow path, and progressive fouling, not equilibrium chemistry alone, govern outcomes remains largely unverified.

In fixed-bed systems, bed depth and flow configuration directly influence contact time, dispersion, and the extent to which reactive sites are accessed before short-circuiting occurs. Deeper beds can improve removal by extending the mass-transfer zone and increasing media inventory, but may also elevate head loss, increase the risk of channelling, and accelerate performance decline under high solids loading (Bulacio Fischer et al., 2025; Quispe et al., 2022). Flow routing strategies can improve distribution and reduce bypass but can also modify biofilm development and clogging dynamics. Broader filtration research, including work on biologically active layers and clogging behaviour, illustrates how coupled physio-chemical and biofilm processes can shape long-term filtration performance and necessitate hydraulic diagnostics in addition to water-quality outcomes (Behjat et al., 2025; Quispe et al., 2023; Reddy et al., 2014; Zakrisson et al., 2024).

Equally important for nutrient applications is stability: adsorption systems can transition from removal to release as media saturate or when water chemistry changes. This issue is well recognized in ion-exchange and mineral media used for ammonium capture, where adsorption–desorption behaviour can be leveraged for recovery but must be quantified to avoid uncontrolled release (Muscarella et al., 2021). For biochar-based systems, regeneration feasibility, operational stability, and end-of-life handling are increasingly considered essential for moving from promising laboratory results to deployable treatment units (Perez-Mercado et al., 2019; Trivedi et al., 2025). Life-cycle assessment studies further show that the sustainability profile of biochar filters depends strongly on production pathways and end-of-life strategies for spent media, emphasizing the value of designing systems with realistic reuse or recovery routes in mind (Osman et al., 2024; Zakrisson et al., 2024).

To close this gap, the present study evaluated Mg^{2+}-activated biochar filtration under continuous flow using real domestic wastewater, focusing on two immediately actionable design levers, which are column hydraulic configuration and bed depth, and linking nutrient performance to hydraulic behaviour and media surface changes over a 30-day operating period. By combining continuous influent–effluent monitoring for ammonium and phosphate with hydraulic assessment (retention and permeability/head loss) and SEM-based surface observations, the work aims to provide engineering evidence that supports scale-up decisions for ammonium polishing and clarifies the operational constraints that must be addressed to achieve stable phosphate capture and recovery in biochar-based filtration systems.

METHOD

Experimental design and reactor configurations

A continuous-flow column study was conducted to evaluate how column configuration and biochar bed depth influence nutrient behaviour in Mg^{2+}-activated biochar filtration. Four column filter units were tested in a 2 × 2 matrix: (i) single-compartment downflow versus (ii) two-compartment downflow–up flow, combined with (iii) Mg-activated biochar bed depths of 25 cm and 50 cm. The two-compartment configuration was created using an internal baffle/partition that forced flow to pass through a downflow section followed by an up-flow section to extend contact and improve distribution. Domestic wastewater was collected from a stabilization pond at a decentralized domestic wastewater treatment facility in Denpasar City and used as the influent feed during the continuous trials. The laboratory scale column filter illustration can be seen below on Figure 1.

Preparation of Mg^{2+}-activated biochar

Biochar was activated with magnesium by soaking the biochar in a magnesium salt solution for 24 hours. The biochar was made from temple waste, wood and coconut fibre waste collected from local waste collection facilities in Denpasar. The waste was pyrolyzed at 500 °C (Wijaya et al, 2025). In the final step, 5 kg of biochar was immersed in an $MgCl_2$ solution (pH 7; 200 mg/L), then drained and oven-dried at 105 °C until constant mass. After drying, the Mg^{2+}-activated biochar was stored in sealed containers at room temperature prior to using. To confirm magnesium loading, biochar samples (before and after activation) were digested with concentrated HNO_3 and H_2SO_4 (5 mL each) and heated until the digestate was clear and free of fumes, indicating complete digestion. Digestates were diluted and analysed for Mg content by flame atomic absorption spectrophotometry (Shimadzu AA-7000F, air–C_2H_2 flame, 285.2 nm), calibrated against a five-point standard curve (0–1.6 ppm, r = 0.9988). AAS a)

b)

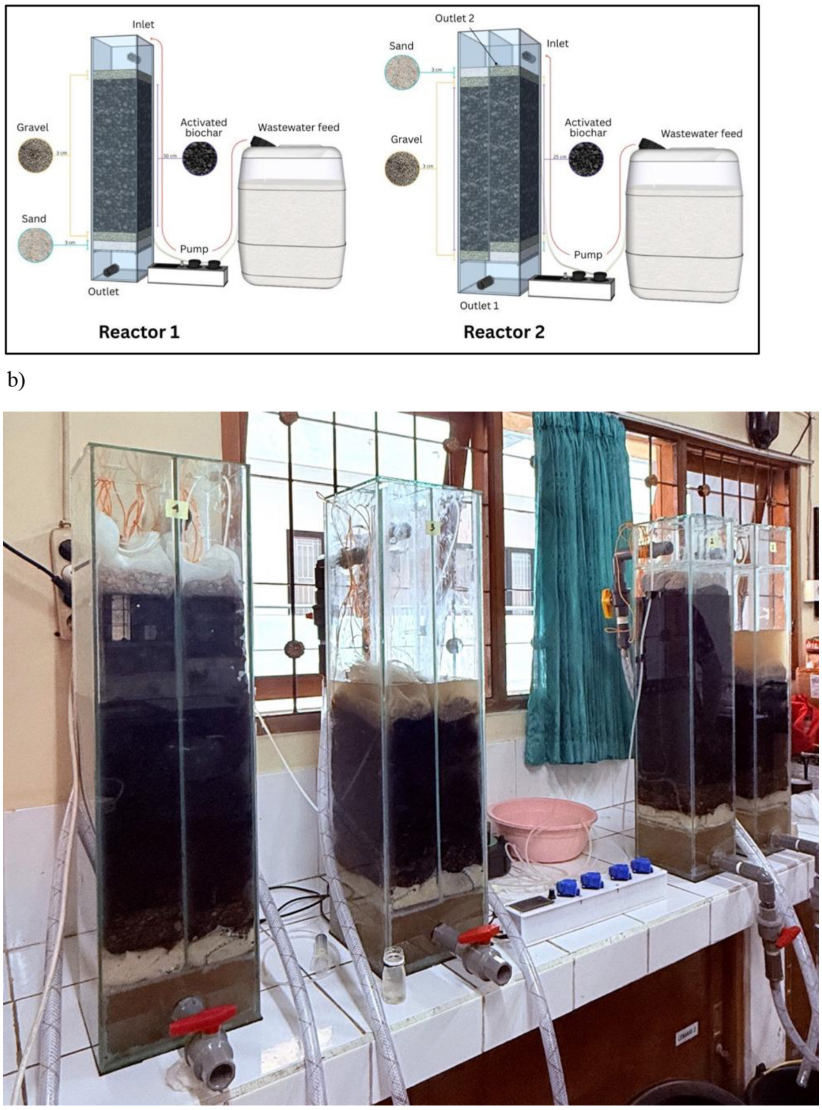

Figure 1. Laboratory-scale column filter reactor: (a) schematic illustration of internal layer configuration and flow path; (b) photograph of the assembled reactors during operation

confirmed successful magnesium loading: Mg content increased from 284.20 ppm in the unactivated biochar to 472.33 ppm after $MgCl_2$ activation, a 66% increase.

Column construction and media packing

Columns were fabricated from acrylic with a rectangular cross-section (20 × 20 cm) and an effective media space height of 60 cm, corresponding to an approximate working volume of 24 L. For each configuration, the packing sequence from bottom to top was fine sand (5 cm), gravel (5 cm), Mg^{2+}-activated biochar (25 and 50 cm), and gravel (5 cm). The sand and gravel layers served as support media to stabilize packing and reduce particle migration, while the Mg^{2+}-activated biochar layer provided the main reactive adsorption zone. Reactor 1 with single column was packed with 25 cm (F1) and 50 cm (F2) of activated biochar. Reactor 2 with two compartments and packed with each 25 cm (F3) and 50 cm (F4) respectively.

Continuous operation and sampling

Wastewater was delivered continuously to the columns using a micropump at a controlled flow rate of approximately 25–30 mL/min. Each unit was operated over a 30-day period. Influent and effluent samples were collected in duplicate at each sampling event and analysed immediately following APHA 4500-NH3/4500-P (Public Health Association, 1992). Sampling was performed on

Table 1. Domestic wastewater sample characteristics

No	Indicators	Unit	Value
1	Total suspended solid	mg/L	29
2	Total dissolved solid	mg/L	759.6
3	pH	-	6–9
4	BOD	mg/L	32.26
5	COD	mg/L	112
6	Ammonia	mg/L	25.8
7	Phosphate	mg/L	8.04
8	Conductivity	µS/cm	1917

30 operational days. Duplicate concentration values were used to calculate the mean and standard deviation reported for each sampling event. The characteristic of domestic wastewater from the stabilization pond (Table 1).

Nutrient analysis

Ammonium and phosphate were quantified by spectrophotometry. Ammonium was measured at 640 nm and phosphate at 880 nm using appropriate colorimetric reagents and calibration standards. Calibration curves were prepared for each analytical batch using multi-point standards covering the expected concentration range. Reagent blanks were included to confirm baseline stability.

Hydraulic performance indicators

Hydraulic indicators were used to interpret treatment behaviour in relation to flow conditions and resistance buildup. Head loss (Δh) across each column was tracked as an operational indicator of resistance development and potential clogging. Headloss was determined from the difference in hydraulic head between inlet and outlet ports.

Hydraulic retention time (HRT) was estimated using:

$$HRT = \frac{V}{Q} \tag{1}$$

where: V is the working volume and Q is the flowing rate. Using $V \approx 24$ L and $Q = 25$ mL/min (1.5 L/h), the representative HRT is approximately 16 h.

Permeability (k) was estimated using Darcy's law:

$$k = \frac{Q \times L}{A \times \Delta h} \tag{2}$$

where: L is the active bed thickness, A is cross-sectional area, and Δh is head loss.

Permeability was used to compare hydraulic behaviour across bed depths and configurations.

SEM analysis of biochar surface morphology

To support interpretation of adsorption and fouling mechanisms, biochar media were collected before operation and after the continuous-flow trials. Samples were dried prior to imaging and examined by scanning electron microscopy (SEM) to evaluate changes in pore structure and surface deposition.

Data processing and performance calculations

Performance was compared across the four configurations using time-series profiles and peak removal periods. Hydraulic indicators (Δh, HRT, and k) were interpreted alongside nutrient results to identify transport limitations and resistance buildup during continuous operation. Removal efficiency was calculated as:

$$Removal\ efficiency = \frac{C_{in} - C_{out}}{C_{in}} \times 100\% \tag{3}$$

where: C_{in} and C_{out} are influent and effluent concentrations (mg/L), respectively.

RESULTS AND DISCUSSION

Four Mg^{2+}-activated biochar filters were operated under continuous flow for 30 days, comparing downflow versus downflow–up flow hydraulics and two biochar bed depths (25 and 50 cm). Overall, ammonium removal showed clear sensitivity to both bed depth and hydraulic configuration, while phosphate behaviour was unstable under continuous operation, with effluent concentrations frequently approaching or exceeding influent values across configurations.

Ammonium removal under continuous Mg^{2+}-activated biochar filtration

All filters exhibited net ammonium removal throughout the 30-day trial, with peak performance consistently occurring early in operation (day 8–9 across all four configurations) followed by a partial decline. For the 25 cm downflow unit (F1), ammonium removal averaged 37.91% ± 17.64% across the monitoring period (mean reduction 20.14 mg/L), with the maximum reduction of 78.38% (42.63 mg/L) observed on day 9; performance declined from an early-phase average of 48.62% (days ≤9) to 26.86% in the later phase (days ≥22). Increasing the bed depth in downflow mode to 50 cm (F2) produced the most temporally consistent removal pattern of the four configurations, averaging 46.34% ± 14.30% overall (peak 77.12% on day 9), with early- and late-phase averages remaining close (46.80% vs. 47.50%), indicating limited decline over the trial. The 25 cm downflow–upflow unit (F3) followed a trend similar to F1, peaking at 76.69% (day 9) and declining from an early-phase average of 55.39% to 29.34% in the later phase, for an overall mean of 44.71% ± 17.24%. The best-performing configuration was the 50 cm downflow–upflow unit (F4), which achieved both the highest overall mean removal (56.29% ± 15.28%) and the highest single-day reduction (79.15%, 46.58 mg/L, day 8); despite a mild decline from 58.00% (early phase) to 48.21% (late phase), F4 maintained the strongest ammonium removal throughout the trial (Figure 2).

Phosphate behaviour and stability in continuous mode

Phosphate exhibited a markedly different, configuration-dependent response than ammonium. The 25 cm downflow unit (F1) achieved stable and effective phosphate removal throughout the entire 30-day trial, averaging 65.03% ± 10.29% (range 38.41–79.61%), with no net-release episodes observed at any sampling point. In contrast, all three remaining configurations displayed an initial period of modest net removal (days 2–6, approximately 3–25% for most days, though F3 reached 49.03% on day 2) followed by an inversion to net phosphate release beginning around day 7, after which effluent concentrations exceeded influent concentrations for most of the remaining trial. This instability was most severe

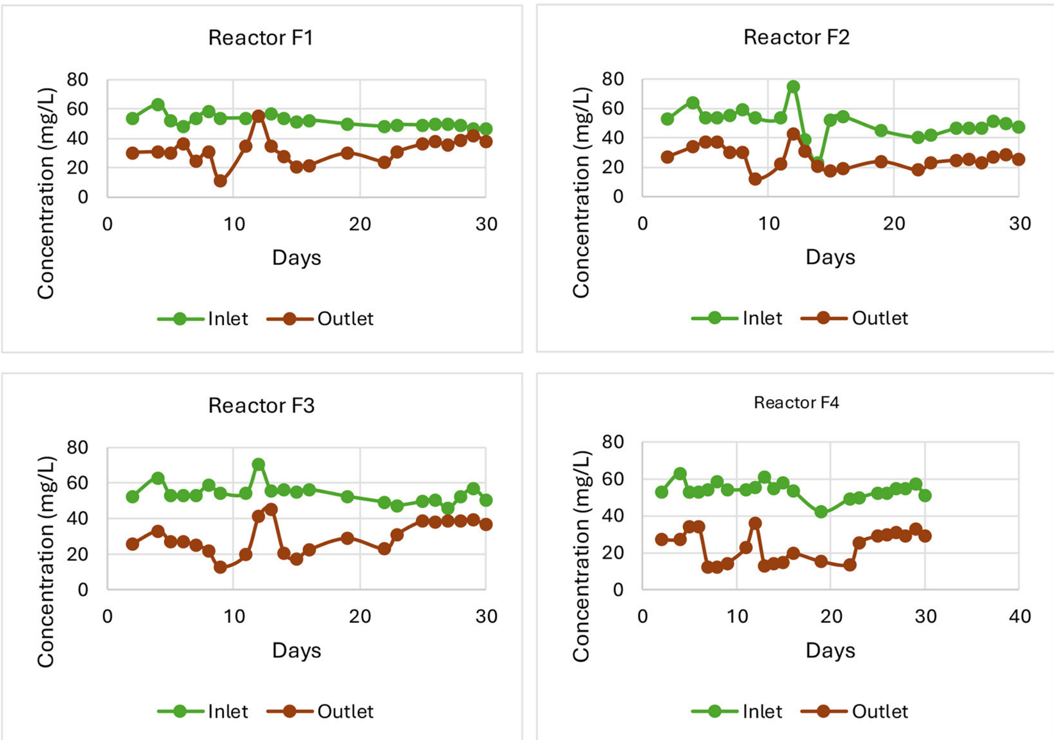

Figure 2. Trends of ammonium concentration in F1, F2, F3, F4

in the 50 cm downflow–upflow unit (F4), which showed the most pronounced and persistent release, averaging −45.88% ± 42.81% and falling below −100% removal on several occasions after day 19. F2 (50 cm, downflow) showed a similarly severe late-stage decline, averaging −33.36% ± 37.28% and reaching −92.86% by day 30. F3 (25 cm, downflow–upflow) displayed the mildest instability of the three unstable configurations, oscillating between modest positive and negative removal through day 12 before trending consistently negative thereafter, for an overall average of −2.60% ± 21.58%. These results indicate that phosphate capture stability was governed less by bed depth alone than by the combination of shallow bed depth and simple downflow hydraulics (F1); increasing bed depth or introducing downflow–upflow staging consistently destabilized phosphate performance (Figure 3).

Operational interpretation of performance over time

Across configurations, ammonium results indicate a consistent early-performance window, with peak removal occurring on day 8 or day 9 in every configuration, followed by reduced net removal as operation progressed. The 50 cm downflow–upflow unit (F4) maintained the highest removal throughout the trial despite this decline, while the 50 cm downflow unit (F2) showed the most temporally consistent performance of the four configurations, with early- and late-phase averages nearly identical. In contrast, phosphate displayed a stable effective removal window in only one configuration: the 25 cm downflow unit (F1) sustained strong phosphate removal throughout the full 30-day trial, while the remaining three configurations (F2, F3, F4) each inverted to net phosphate release after approximately one week of operation. This indicates that phosphate capture stability was strongly dependent on filter configuration rather than being uniformly unsustainable across the system.

Hydraulic indicators: retention and permeability

The representative hydraulic retention time for the laboratory-scale system was approximately 16 h at a flow rate of 25 mL/min (working

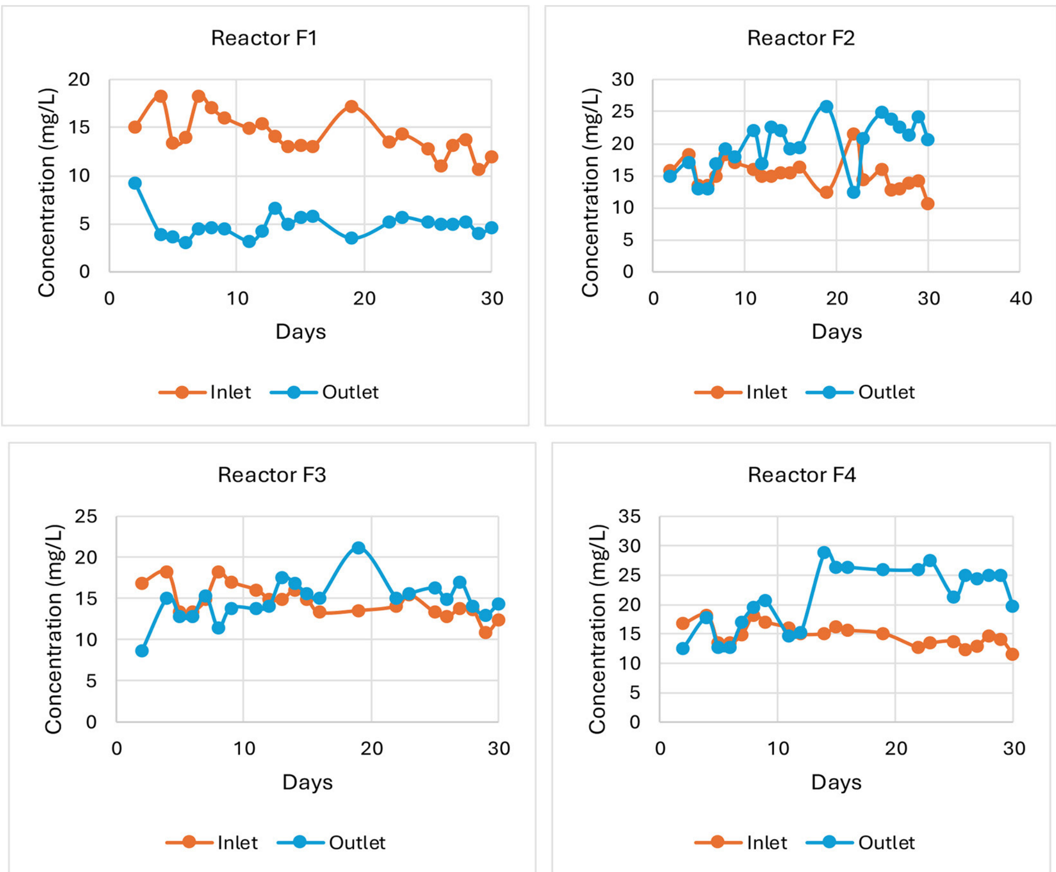

Figure 3. Trends of phosphate concentration in F1, F2, F3, F4

volume ≈ 24 L). Permeability was estimated using Darcy-based calculations. Under the same calculation approach, the 25 cm biochar-bed systems (F1 and F3; total media thickness 0.40 m) yielded an estimated permeability of 0.000714 cm/s, while the 50 cm bed systems (F2 and F4; total media thickness 0.65 m) yielded an estimated permeability of 0.001161 cm/s. These estimates indicate that bed depth and the assumed head-loss term strongly influence the derived permeability values used for comparative interpretation.

SEM evidence of media surface evolution during operation

SEM observations showed pronounced changes in surface morphology after continuous operation. Previous study has presented the fresh Mg^{2+}-activated biochar exhibited open, heterogeneous pore networks and relatively clean pore walls (I. Wijaya, 2025). After filtration, the media surfaces showed substantial pore blockage and deposited materials, including fine particulates and amorphous layers occupying pore entrances and internal channels. The observed transition is consistent with progressive fouling and reduced accessible porosity during continuous operation, which aligns with the time-dependent shifts observed in nutrient removal performance (Figures 4, 5).

Mg^{2+}-activated biochar filtration achieved robust and design-responsive ammonium removal, with maximum reductions ranging from 57% to 79%. The highest peak performance and the most stable later-stage behavior were obtained with the 50 cm downflow–upflow configuration (F4). Phosphate behavior was unstable in continuous mode across all configurations, frequently exhibiting effluent concentrations above influent. Hydraulic estimates and SEM observations collectively indicate that media thickness and progressive pore blockage/fouling are important operational factors shaping long-run performance.

DISCUSSION

The continuous-flow results highlight a key practical distinction between nutrient removal observed under controlled adsorption tests and the behaviour that emerges when reactive media are operated as unit processes. Across all configurations, ammonium removal showed a clear early-performance window followed by declining or stabilizing removal, which is consistent with fixed-bed systems where a high initial driving

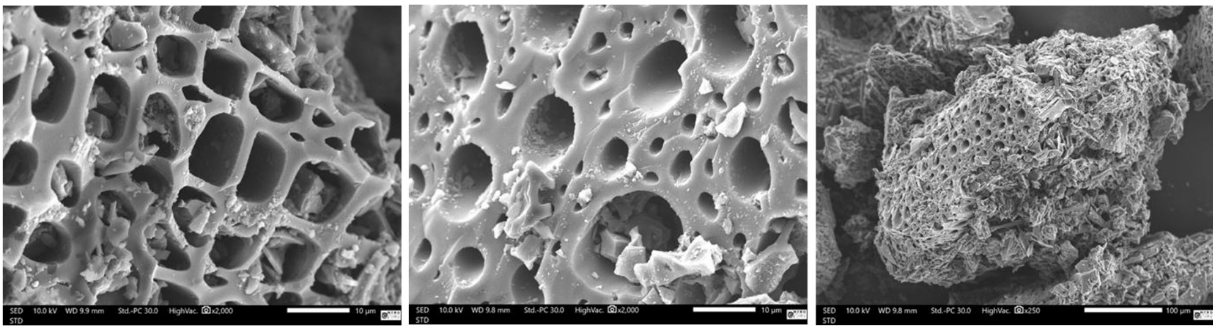

Figure 4. SEM analysis for the 25 cm biochar medium

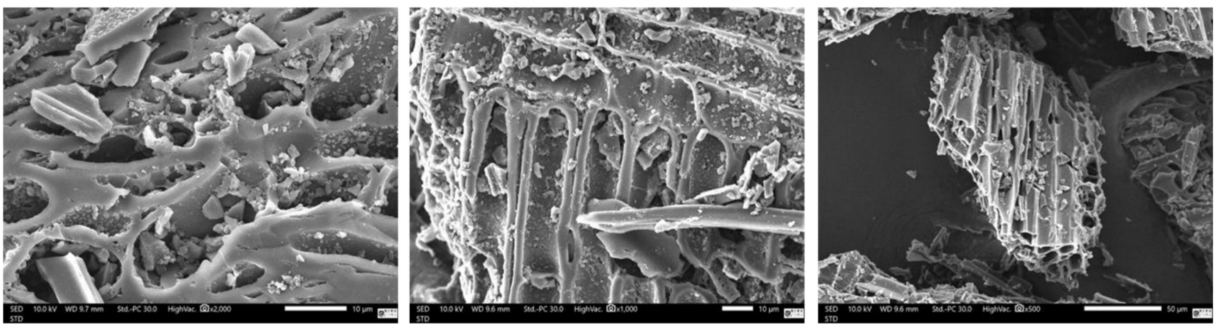

Figure 5. SEM analysis for the 50 cm biochar medium

force and abundant available sites gradually give way to site occupation, intraparticle diffusion limits, and changing surface chemistry over time (Baaloudj et al., 2025; Zhang et al., 2025). This outcome reinforces calls from recent reviews that emphasize the need to validate biochar performance in process-relevant modes (e.g., column filtration) rather than relying predominantly on batch datasets, especially when the intended application is continuous treatment or polishing (Jagadeesh and Sundaram, 2023; Quispe et al., 2022; Trivedi et al., 2025).

In contrast, phosphate did not show sustained net removal and frequently exhibited effluent concentrations above influent. Similar discrepancies between batch expectations and column performance are increasingly reported for engineered adsorbents when real wastewater matrices introduce competing ions, particulate retention, and biological activity that alter apparent removal signals (Perez-Mercado et al., 2019; Quispe et al., 2022). The phosphate behavior is therefore not a peripheral issue; it is a central operational finding that clarifies the boundary conditions under which Mg^{2+}-activated biochar filtration can be deployed as a reliable nutrient control step.

How bed depth and hydraulic staging improved ammonium performance

Two design levers produced consistent directional improvements for ammonium: increased bed depth and staged downflow–up flow hydraulics. A deeper bed increases reactive media inventory and expands the mass-transfer zone, reducing the likelihood that ammonium exits the column before contacting active sites. Staged routing (downflow followed by up flow) can improve flow distribution and mitigate short-circuiting, which becomes increasingly important as pore networks evolve during operation and preferential pathways develop(Quispe et al., 2022; Susilawati et al., 2023). The superior peak and later-stage behaviour of the deeper staged configuration is therefore consistent with fixed-bed design principles and with recent work showing that optimized downflow fixed-bed systems can sustain treatment performance longer when hydrodynamics and media accessibility are addressed explicitly (Baaloudj et al., 2025).

Mechanistically, ammonium capture on biochar is typically associated with cation exchange, electrostatic attraction to oxygen-containing functional groups, and interactions with mineral phases introduced during modification (Jagadeesh and Sundaram, 2023; Jiang et al., 2019). Mg loading is expected to enhance surface reactivity and alter ionic interactions, and feedstock-dependent studies have shown that Mg-modified biochars can substantially improve nutrient adsorption relative to unmodified materials, though with high sensitivity to material properties and operational conditions (Jiang et al., 2019). At the same time, several assessments caution that ammonium sorption capacities reported for biochar can be overestimated when conditions are idealized or when competing processes are not accounted for, underscoring the value of continuous-flow evidence like that provided here (Weldon et al., 2022).

Interpreting phosphate instability in continuous mode

Phosphate capture was not uniformly unstable across configurations: the 25 cm downflow unit (F1) sustained effective removal throughout the 30-day trial, whereas the remaining three configurations (F2, F3, F4) each transitioned from modest early removal to recurring net phosphate release after approximately one week of operation. Several non-exclusive mechanisms can plausibly explain both the instability observed in F2–F4 and its absence in F1. First, phosphate desorption can occur if binding is dominated by weak electrostatic interactions that are sensitive to pH, ionic strength, or competition from bicarbonate, sulphate, and dissolved organics typical of domestic wastewater (Jagadeesh and Sundaram, 2023; Quispe et al., 2022). Second, physically retained particulate or organic phosphorus can be mineralized within the bed, releasing orthophosphate downstream and producing apparent "negative removal" even if some adsorption is occurring simultaneously (Bai et al., 2024; Quispe et al., 2022). Third, biofilm growth can temporarily immobilize phosphorus and later release it through sloughing, lysis, or changing microenvironments, phenomena widely recognized in filtration systems where biologically active layers develop during continuous operation (Bai et al., 2024; Quispe et al., 2022; Verma et al., 2024).

All three mechanisms would be expected to intensify with greater bed depth and with downflow–upflow staging: a deeper bed retains solids and biomass for longer, extending the residence time available for biofilm development and mineralization, while upflow staging increases hydraulic mixing and contact with previously deposited material. This is consistent with F1 (the shallowest bed, simplest downflow path) remaining stable while F2–F4 destabilized. This contrast with the literature is most informative when viewed alongside the divergence between configurations: batch equilibrium studies of Mg-loaded biochar report substantial net phosphate uptake (up to 116 mg P/g in Xu et al., 2018; up to 31 mg P/g in Jiang et al., 2019), yet under continuous flow with real domestic wastewater the same Mg-activation chemistry produced net phosphate release in three of the four tested configurations (F2–F4). A shaken-batch equilibrium test is structurally unable to surface this behaviour, since desorption and leaching dynamics only emerge as flow, bed saturation, and biological activity evolve over sustained operation — underscoring why the continuous-flow evaluation performed here is necessary, not merely incremental, for assessing deployment readiness. Notably, F1's sustained removal shows that this batch-to-continuous gap is not universal but configuration-dependent, reinforcing the case for testing candidate designs under realistic hydraulic conditions rather than assuming batch-derived capacities will translate directly to field performance. From a design standpoint, these results suggest that Mg^{2+} activation alone is not sufficient to guarantee stable phosphate capture in real-wastewater columns, and that process controls and/or hybrid media strategies are needed. This aligns with broader nutrient recovery literature emphasizing that engineered biochar can support nutrient capture, but performance and stability depend strongly on how the system manages equilibrium shifts and media saturation during operation (Marcińczyk et al., 2022; Wu and Vaneeckhaute, 2022). Practically, conditioning protocols (pre-washing/leaching tests), operational monitoring (pH and conductivity), and layered-bed designs that add a stronger phosphate-selective sorbent stage are reasonable next-step pathways to convert phosphate instability into a controllable recovery route (Samaraweera et al., 2023; Wu and Vaneeckhaute, 2022; Zeng et al., 2013).

Fouling, pore accessibility, and why performance changes over time

SEM micrographs of the spent Mg^{2+}-activated biochar recovered after continuous filtration showed a clear depth-dependent evolution of pore accessibility and surface deposition. The biochar from the 25 cm bed largely retained its plant-derived cellular architecture, with a well-defined macropore network and many pore mouths remaining open. At higher magnification, deposits were present but appeared mainly as localized particulate attachments within pores and along pore edges rather than as a continuous coating. This morphology suggests that a substantial fraction of the internal pore volume and reactive surface remained accessible to flow and diffusion, supporting sustained contact between dissolved nutrients and adsorption sites during the early operating period.

In contrast, the biochar collected from the 50 cm bed exhibited more extensive surface coverage and pore occlusion. Compared at similar magnifications, pore throats were more frequently narrowed or blocked by granular deposits and fine particulates, and the pore walls appeared more heavily coated. Plate-like fragments and clustered aggregates were also more prominent, indicating stronger accumulation of retained solids and/or precipitated phases within the deeper bed. These features imply a reduction in effective porosity and increased tortuosity, which can constrain intraparticle diffusion and shift the system toward transport-limited behavior during prolonged operation.

Overall, the SEM comparison indicates that increasing bed depth from 25 cm to 50 cm can intensify fouling and pore blockage under continuous real-wastewater loading, likely because deeper beds provide a larger capture volume for suspended solids and a longer residence time for deposition, biofilm development, and secondary phase formation. Such depth-associated pore occlusion is consistent with broader observations in biochar-based column filtration and other porous-media filtration systems, where long-run performance is often governed by clogging, surface coating, and evolving hydraulics rather than only intrinsic adsorption capacity (Baaloudj et al., 2025; Bai et al., 2024; Quispe et al., 2022). This morphological evidence provides a plausible structural basis for time-dependent shifts in nutrient removal during continuous operation and highlights the practical importance of solids pre-treatment, bed design, and regeneration/replacement planning when implementing deeper biochar beds in engineered filtration units (Baaloudj et al., 2025; Jagadeesh and Sundaram, 2023; Trivedi et al., 2025).

Implications for engineering deployment and nutrient recovery

The results support Mg^{2+}-activated biochar filtration as a promising polishing option for ammonium, especially when implemented with sufficient bed depth and hydraulics that reduce short-circuiting. For practical deployment, the findings imply that upstream solids management (e.g., settling/screening) and operational strategies to slow fouling are likely to extend effective media lifetime, consistent with filtration literature that links solids loading to clogging rates and performance decay (Bai et al., 2024).

For phosphate, the main implication is that stability must be designed rather than assumed. Options include (i) media conditioning and leaching control to reduce release artifacts; (ii) operational control of pH/ionic strength; (iii) layered or hybrid beds that include a dedicated phosphate-selective stage; and (iv) recovery-oriented coupling where mobilized phosphate is captured downstream in a controlled precipitation or adsorption unit (Gao et al., 2024; Marcińczyk et al., 2022). Importantly, this aligns with sustainability and circularity considerations: if spent biochar is intended for beneficial reuse (e.g., as a soil amendment), both nutrient retention stability and environmental trade-offs must be evaluated, as highlighted in life cycle and systems analyses of biochar filtration concepts (Behjat et al., 2025; Osman et al., 2024; Wu and Vaneeckhaute, 2022).

Proximate analysis of the spent (post-adsorption) biochar recovered from this study supports this reuse potential: across the four reactors, the used media retained 0.29% N, 710.23 mg/kg P, and 9042.56 mg/kg K, with 28.88% organic carbon (C/N ratio 99.59), indicating meaningful nutrient enrichment alongside a carbon-rich matrix consistent with soil amendment value.

Study limitations and next research

Three limitations shape the interpretation and define priority next experiments. First, phosphate stability is difficult to resolve mechanistically without concurrent monitoring of pH, conductivity/alkalinity, and dissolved organic matter, which are known to influence phosphate binding and release pathways in engineered sorbent systems. Second, fixed-bed comparisons are strengthened by reporting breakthrough behaviour in normalized units (e.g., bed volumes treated) and by including replicate runs or repeated cycles to quantify variability in real wastewater operation. Third, proximate characterization (N, P, K, organic carbon) was performed only on the spent biochar recovered after continuous operation; corresponding analysis of the fresh, pre-activation material was not conducted in this study, which limits direct attribution of nutrient enrichment to adsorption versus baseline feedstock composition.

Future work should therefore (i) couple nutrient time series with pH and conductivity tracking to diagnose release drivers; (ii) report performance as both concentrations and cumulative mass removal versus bed volumes; (iii) test conditioning and regeneration protocols to quantify controlled desorption and recovery potential, drawing on established adsorption–desorption frameworks from ion-exchange column systems (Konneh et al., 2021; Muscarella et al., 2021); and (iv) evaluate layered-bed or hybrid configurations explicitly designed to stabilize phosphate capture while preserving ammonium polishing performance [8,16].

Overall, Mg^{2+}-activated biochar columns demonstrated robust ammonium removal with clear sensitivity to bed depth and hydraulic staging, supporting their potential role as modular polishing units. Phosphate behaviour, however, was unstable under continuous real-wastewater operation, indicating that reliable P capture will require additional controls or hybridization. By linking nutrient trends with hydraulic and SEM evidence, the study clarifies both the opportunity (ammonium polishing) and the constraint (phosphate stability) that must be addressed to translate Mg^{2+}-activated biochar filtration from promising material concept to dependable treatment and recovery technology in practice.

Acknowledgments

The authors thank to Badan Riset dan Inovasi Nasional (BRIN) Republik Indonesia for funding this research under Riset Inovasi untuk Indonesia Maju (RIIM) program (Contract No. 224/IV/KS/10/2025).

REFERENCES

1. Baaloudj, O., Langerame, F., Iunnissi, R., Buttiglieri, G., Buono, D. Del, Khadhar, S., … Brienza, M. (2025). Biochar-based downflow fixed-bed adsorption systems for water treatment: process optimization, reusability, and techno-economic evaluation. *Separation and Purification Technology*, *377*. https://doi.org/10.1016/j.seppur.2025.134347
2. Bai, X., Samari-Kermani, M., Schijven, J., Raoof, A., Dinkla, I. J. T., Muyzer, G. (2024). Enhancing slow sand filtration for safe drinking water production: interdisciplinary insights into Schmutzdecke characteristics and filtration performance in mini-scale filters. *Water Research*, *262*. https://doi.org/10.1016/j.watres.2024.122059
3. Balkrishna, A., Kaushik, P., Singh, S., Agrahari, P., Kumar, B., Kumar, P., Arya, V. P. (2025, March 1). Potential use of sewage sludge as fertilizer in organic farming. *Cleaner Waste Systems*, *10*. Elsevier B.V. https://doi.org/10.1016/j.clwas.2025.100245
4. Behjat, M., Svanström, M., Peters, G., Wennberg, N. (2025). Life cycle assessment of recirculating aquaculture systems with innovative biochar filter for enhanced nutrient recirculation. *Resources, Environment and Sustainability*, *21*. https://doi.org/10.1016/j.resenv.2025.100233
5. Bulacio Fischer, P. T., Di Trapani, D., Laudicina, V. A., Mineo, A., Muscarella, S. M., Mannina, G. (2025). Adsorption and desorption of ammonium from treated wastewater by zeolite filled columns: An experimental study at the water resource recovery facility of Palermo University – Italy. *Journal of Environmental Management*, *375*. https://doi.org/10.1016/j.jenvman.2025.124241
6. Czuba, K., Bastrzyk, A., Rogowska, A., Janiak, K., Pacyna, K., Kossińska, N., … Podstawczyk, D. (2021). Towards the circular economy — A pilot-scale membrane technology for the recovery of water and nutrients from secondary effluent. *Science of the Total Environment*, *791*. https://doi.org/10.1016/j.scitotenv.2021.148266
7. Gao, Y., Wang, J., Ge, Y., Lei, Y., Wei, X., Xu, Y., Zheng, X. (2024). Partial substitution of nitrogen fertilizers by organic products of rural waste co-composting impacts on farmland soil quality. *Environmental Technology and Innovation*, *33*. https://doi.org/10.1016/j.eti.2023.103470
8. Goldschmidt, A., Buffam, I. (2023). Biochar-amended substrate improves nutrient retention in green roof plots. *Nature-Based Solutions*, *3*, 100066. https://doi.org/10.1016/j.nbsj.2023.100066
9. Gong, Y. P., Ni, Z. Y., Xiong, Z. Z., Cheng, L. H., Xu, X. H. (2017). Phosphate and ammonium adsorption of the modified biochar based on Phragmites australis after phytoremediation. *Environmental Science and Pollution Research*, *24*(9), 8326–8335. https://doi.org/10.1007/s11356-017-8499-2
10. Ha, T. H., Mahasti, N. N. N., Lu, M. C., Huang, Y. H. (2023). Ammonium-nitrogen recovery as struvite from swine wastewater using various magnesium sources. *Separation and Purification Technology*, *308*. https://doi.org/10.1016/j.seppur.2022.122870
11. Hartati, W., Serlyani, S., Syahrinudin, Sudarmadji, T. (2025). Optimizing biochar application: Impact on soil chemical properties in spodosols and ultisols. *Ecological Engineering and Environmental Technology*, *26*(3), 95–110. https://doi.org/10.12912/27197050/199535
12. Hofmann, A. H., Liesegang, S. L., Keuter, V., Eticha, D., Steinmetz, H., Katayama, V. T. (2024). Nutrient recovery from wastewater for hydroponic systems: A comparative analysis of fertilizer demand, recovery products, and supply potential of WWTPs. *Journal of Environmental Management*, *352*. https://doi.org/10.1016/j.jenvman.2023.119960
13. Jagadeesh, N., Sundaram, B. (2023). Adsorption of pollutants from wastewater by biochar: A review. *Journal of Hazardous Materials Advances*, *9*. https://doi.org/10.1016/j.hazadv.2022.100226
14. Jiang, Y. H., Li, A. Y., Deng, H., Ye, C. H., Wu, Y. Q., Linmu, Y. D., Hang, H. L. (2019). Characteristics of nitrogen and phosphorus adsorption by Mg-loaded biochar from different feedstocks. *Bioresource Technology*, *276*, 183–189. https://doi.org/10.1016/j.biortech.2018.12.079
15. Konneh, M., Wandera, S. M., Murunga, S. I., Raude, J. M. (2021). Adsorption and desorption of nutrients from abattoir wastewater: modelling and comparison of rice, coconut and coffee husk biochar. *Heliyon*, *7*(11). https://doi.org/10.1016/j.heliyon.2021.e08458
16. Kundu, S., Vassanda Coumar, M., Rajendiran, S., Ajay, Subba Rao, A. (2015). Phosphates from detergents and eutrophication of surface water ecosystem in India. *Current Science*, *108*(7), 1320–1325.
17. Mahmoud, E. K. (2018). Textile wastewater treatment by using cement kiln dust and biochar filter. *Desalination and Water Treatment*, *120*, 180–184. https://doi.org/10.5004/dwt.2018.22744
18. Marcińczyk, M., Ok, Y. S., Oleszczuk, P. (2022, November 1). From waste to fertilizer: Nutrient recovery from wastewater by pristine and engineered biochars. *Chemosphere*, *306*. Elsevier Ltd. https://doi.org/10.1016/j.chemosphere.2022.135310
19. Muscarella, S. M., Badalucco, L., Cano, B., Laudicina, V. A., Mannina, G. (2021). Ammonium adsorption, desorption and recovery by acid and alkaline treated zeolite. *Bioresource Technology*, *341*. https://doi.org/10.1016/j.biortech.2021.125812
20. Nehhal, S., Ben Ali, M., Abrouki, Y., Ofqir, K., Elkahoui, Y., El Hajjaji, S. (2025). Sustainable

conversion of agricultural waste to activated biochar: Optimization and modelling of methylene blue adsorption. *Ecological Engineering and Environmental Technology*, *26*(12), 302–320. https://doi.org/10.12912/27197050/214189

21. Nika, C. E., Vasilaki, V., Expósito, A., Katsou, E. (2020). Water cycle and circular economy: developing a circularity assessment framework for complex water systems. *Water Research*, *187*. https://doi.org/10.1016/j.watres.2020.116423
22. Osman, A. I., Farghali, M., Rashwan, A. K. (2024). Life cycle assessment of biochar as a green sorbent for soil remediation. *Current Opinion in Green and Sustainable Chemistry*, 100882. https://doi.org/10.1016/j.cogsc.2024.100882
23. Panjwani, A. A., Cowan, A. E., Jun, S., Bailey, R. L. (2021). Trends in nutrient- and non-nutrient–containing dietary supplement use among US children from 1999 to 2016. *Journal of Pediatrics*, *231*, 131–140.e2. https://doi.org/10.1016/j.jpeds.2020.12.021
24. Perez-Mercado, L. F., Lalander, C., Joel, A., Ottoson, J., Dalahmeh, S., Vinnerås, B. (2019). Biochar filters as an on-farm treatment to reduce pathogens when irrigating with wastewater-polluted sources. *Journal of Environmental Management*, *248*. https://doi.org/10.1016/j.jenvman.2019.109295
25. Public Health Association, A. (1992). *APHA Method 4500-P: Standard Methods for the Examination of Water and Wastewater*.
26. Quispe, J. I. B., Campos, L. C., Mašek, O., Bogush, A. (2022, August 1). Use of biochar-based column filtration systems for greywater treatment: A systematic literature review. *Journal of Water Process Engineering*, *48*. Elsevier Ltd. https://doi.org/10.1016/j.jwpe.2022.102908
27. Quispe, J. I. B., Campos, L. C., Mašek, O., Bogush, A. (2023). Optimisation of biochar filter for handwashing wastewater treatment and potential treated water reuse for handwashing. *Journal of Water Process Engineering*, *54*. https://doi.org/10.1016/j.jwpe.2023.104001
28. Reddy, K. R., Nagaraja, B., Palomino, A. M. (2025). Chitosan–biochar composite for environmental remediation: enhanced phosphate removal from stormwater. *Lecture Notes in Civil Engineering*, *659 LNCE*, 11–24. Springer Science and Business Media Deutschland GmbH. https://doi.org/10.1007/978-981-96-8536-3_2
29. Reddy, K. R., Xie, T., Dastgheibi, S. (2014). Evaluation of biochar as a potential filter media for the removal of mixed contaminants from urban storm water runoff. *Journal of Environmental Engineering*, *140*(12). https://doi.org/10.1061/(asce)ee.1943-7870.0000872
30. Ren, T., Fan, P., Zuo, W., Liao, Z., Wang, F., Wei, Y., … Liu, G. (2023). Biochar-based fertilizer under drip irrigation: More conducive to improving soil carbon pool and promoting nitrogen utilization. *Ecological Indicators*, *154*. https://doi.org/10.1016/j.ecolind.2023.110583
31. Rey-Martínez, N., Torres-Sallan, G., Morales, N., Serra, E., Bisschops, I., van Eekert, M. H. A., … Sanchis, S. (2024). Combination of technologies for nutrient recovery from wastewater: A review. *Cleaner Waste Systems*, *7*. https://doi.org/10.1016/j.clwas.2024.100139
32. Ricklefs-Johnson, K., Pikosky, M. A., Cifelli, C. J., Fulgoni, K., Fulgoni, V. L., Agarwal, S. (2023). Assessment of beverage trends and replacing non-dairy caloric beverages with milk at meals across childhood improves intake of key nutrients at risk of inadequate consumption: An NHANES modeling study. *Current Developments in Nutrition*, *7*(11). https://doi.org/10.1016/j.cdnut.2023.102020
33. Samaraweera, H., Palansooriya, K. N., Dissanayaka, P. D., Khan, A. H., Sillanpää, M., Mlsna, T. (2023). Sustainable phosphate removal using Mg/Ca-modified biochar hybrids: Current trends and future outlooks. *Case Studies in Chemical and Environmental Engineering*, *8*. https://doi.org/10.1016/j.cscee.2023.100528
34. Slootweg, J. C. (2020, June 1). Using waste as resource to realize a circular economy: Circular use of C, N and P. *Current Opinion in Green and Sustainable Chemistry*, *23*, 61–66. Elsevier B.V. https://doi.org/10.1016/j.cogsc.2020.02.007
35. Susilawati, Sihombing, Y. A., Rahayu, S. U., Sembiring, Y. Y. B., Waldiansyah, L., Irma, M. (2023). Filter material based on zeolite-activated charcoal from cocoa shells as ammonium adsorbent in greywater treatment. *South African Journal of Chemical Engineering*, *43*, 266–272. https://doi.org/10.1016/j.sajce.2022.11.006
36. Trivedi, Y., Sharma, M., Mishra, R. K., Sharma, A., Joshi, J., Gupta, A. B., … Vuppaladadiyamd, A. K. (2025, May 1). Biochar potential for pollutant removal during wastewater treatment: A comprehensive review of separation mechanisms, technological integration, and process analysis. *Desalination*, *600*. Elsevier B.V. https://doi.org/10.1016/j.desal.2024.118509
37. Ural-Janssen, A., Kroeze, C., Meers, E., Strokal, M. (2024). Large reductions in nutrient losses needed to avoid future coastal eutrophication across Europe. *Marine Environmental Research*, 106446. https://doi.org/10.1016/j.marenvres.2024.106446
38. Verma, A., Yalem, R., Saini, G. (2024). Use of recycled aggregates as filter support and filter media for decentralized water filtration systems. *Journal of Engineering Research (Kuwait)*. https://doi.org/10.1016/j.jer.2023.10.016
39. Weldon, S., van der Veen, B., Farkas, E.,

Kocatürk-Schumacher, N. P., Dieguez-Alonso, A., Budai, A., Rasse, D. (2022, August 1). A re-analysis of NH4+ sorption on biochar: Have expectations been too high? *Chemosphere*, *301*. Elsevier Ltd. https://doi.org/10.1016/j.chemosphere.2022.134662

40. Wijaya, I. (2025). Adsorption Kinetics and Isotherm Study of Ammonium and Phosphate Removal Using Mg2+-Activated Biochar. *Journal of Ecological Engineering*, *26*(6), 62–75. https://doi.org/https://doi.org/10.12911/22998993/201996
41. Wijaya, I. M. W., Partama, I. G. Y., Sumantra, I. K. (2023). Study on Nutrients Concentration Trends in Tukad Badung River Toward Nutrient Recovery Potential. *IOP Conference Series: Earth and Environmental Science*, *1268*(1), 012002. https://doi.org/10.1088/1755-1315/1268/1/012002
42. Wijaya, I., Yudha Partama, I. G., Ketut Sumantra, I., Deoram Ahire, K., Vebrian Kenedy, F. (2025). Nutrient dynamics and recovery potential in the Tukad Badung River, Indonesia. *Nature Environment and Pollution Technology*, *24*(3). https://doi.org/10.46488/NEPT.2025.v24i03.D1750
43. Wu, H., Foster, X., Kazemian, H., Diby, I. C. P., Kaliaguine, S., Vaneeckhaute, C. (2025). Nutrient recovery from urine: Urea adsorption onto biochar integrated with Na-chabazite as urease inhibitor. *Resources, Conservation and Recycling*, *212*. https://doi.org/10.1016/j.resconrec.2024.107955
44. Wu, H., Vaneeckhaute, C. (2022, April 1). Nutrient recovery from wastewater: A review on the integrated Physicochemical technologies of ammonia stripping, adsorption and struvite precipitation. *Chemical Engineering Journal*, *433*. Elsevier B.V. https://doi.org/10.1016/j.cej.2021.133664
45. Xu, K., Lin, F., Dou, X., Zheng, M., Tan, W., Wang, C. (2018). Recovery of ammonium and phosphate from urine as value-added fertilizer using wood waste biochar loaded with magnesium oxides. *Journal of Cleaner Production*, *187*, 205–214. https://doi.org/10.1016/j.jclepro.2018.03.206
46. Yu, Y., Lu, X., Wu, Y. (2014). Performance of an anaerobic baffled filter reactor in the treatment of algae-laden water and the contribution of granular sludge. *Water (Switzerland)*, *6*(1), 122–138. https://doi.org/10.3390/w6010122
47. Zakrisson, L., Sundberg, C., Larsson, G., Azzi, E. S., Dalahmeh, S. S. (2024). Life cycle assessment of biochar filters for on-site wastewater treatment. *Journal of Environmental Management*, *371*. https://doi.org/10.1016/j.jenvman.2024.123265
48. Zeng, Z., Zhang, S. Da, Li, T. Q., Zhao, F. L., He, Z. L., Zhao, H. P., … Rafiq, M. T. (2013). Sorption of ammonium and phosphate from aqueous solution by biochar derived from phytoremediation plants. *Journal of Zhejiang University: Science B*, *14*(12), 1152–1161. https://doi.org/10.1631/jzus.B1300102
49. Zhang, H., Zou, Q., Liu, X., Ning, X., Wang, J., Zhang, H., Yang, Y. (2025). Transforming waste into resource: Ammonia plasma-modified biochar for efficient phosphate removal and fertilizer use in rice cultivation. *Industrial Crops and Products*, *236*. https://doi.org/10.1016/j.indcrop.2025.121894